

FLOW AND PLASTICITY VIA NONEQUILIBRIUM MOLECULAR DYNAMICS

WILLIAM G. HOOVER

1. SYNOPSIS

The viscous flow of fluids and the plastic flow of solids, such as metals, are interesting from both the practical and the theoretical points of view. Atomistic "molecular dynamics" simulations provide a way of visualizing and understanding these flows in a detailed microscopic way. Simulations are necessarily carried out at relatively high rates of strain. For this reason they are ideally suited to the study of nonlinear flow phenomena: normal stresses induced by shear deformation, stress rotation, and the coupling of stress with heat flow, for instance. The simulations require appropriate boundary conditions, forces, and equations of motion. Newtonian mechanics is relatively inefficient for this simulation task. A modification, "Nonequilibrium Molecular Dynamics," has been developed to simulate nonequilibrium flows.<sup>1</sup> By now, many high-strain-rate rheological studies of flowing (viscous) fluids and (plastic) solids have been carried out. Here I describe the new methods used in the simulations and some results obtained in this way. A three-body shear-flow exercise is appended to make these ideas more concrete.

G. Jacucci (ed.), *Computer Simulation in Physical Metallurgy*, 87-106.  
 © 1986 ECSC, EEC, EAEC, Brussels and Luxembourg.

## 2. INTRODUCTION

Molecular dynamics is the numerical solution of the equations of motion of  $N$  interacting particles. The original "equilibrium" version of molecular dynamics solved Newton's equations of motion. The volume  $V$  was kept fixed, so that the energy  $E$  was a constant of the motion. This early work was mainly devoted to determining the thermodynamic "equation of state", relating the pressure  $P$  and temperature  $T$  to  $E$  and  $V$ . A few studies of linear transport phenomena were carried out, using expressions linking equilibrium fluctuations to linear transport properties. Velocity fluctuations, stress fluctuations, and heat current fluctuations respectively were used to find the diffusion coefficient, the viscosity coefficients, and the thermal conductivity. In addition, the structure of fluids, including gas-liquid mixtures, and the dynamic approach to equilibrium were studied. The equilibrium results led to theoretical advances in estimating the equation of state. Results for simple systems were used as a basis for a perturbation treatment of more complicated cases. This approach was successful. The equation-of-state problem can now be considered solved, at least for simple, pairwise-additive short-ranged interactions.

Progress on nonequilibrium problems has been slower due to the lack of a suitable perturbation theory. For this reason there has been considerable activity in simulating, as opposed to calculating from theory, nonequilibrium flows. Shockwaves, surface collisions, rapid expansions, heat flows, and the like have all been studied. Here I will describe only the shear deformation of simple materials (either fluid or solid), a path leading to viscosity for fluids<sup>2</sup> and to yield strength for solids.<sup>3</sup>

These simulations use a modified "nonequilibrium" molecular dynamics which incorporates the deformation being studied as well as a steady-state

thermostat to increase computational efficiency. I describe the thermostatting and deformation techniques first. Then I outline the applications of these nonequilibrium techniques to particular fluid and solid systems.

I believe there is great potential for combining the nonequilibrium methods with models for metals to study problems of metallurgical interest. This application of nonequilibrium molecular dynamics is still in its infancy.

### 3. NONEQUILIBRIUM MOLECULAR DYNAMICS

Irreversible flows invariably involve the conversion of work into heat. The irreversible heat then acts to change material properties in a very nonlinear way. Thus transient irreversible problems are much more complicated than steady flows. The irreversible heating is particularly severe in microscopic computer simulations because very high strain rates must be used. (Otherwise the simulations would require too much time.) Gigahertz to terahertz strain rates are necessary if the induced stresses are to exceed the natural thermal fluctuations present in small systems. Thus the time required for a significant change in shape in a computer simulation lies between a picosecond and a nanosecond.

A nanosecond of real time corresponds to about 100,000 time steps in a computer simulation. Terahertz strain rates exceed the rates in rapid Hopkinson-bar experiments by about seven orders of magnitude. Because the irreversible heat varies as the square of the deformation rate, the heating rate in a straightforward computer simulation would be of order  $10^{12}$  kelvins/second.

To avoid the irreversible heating, steady states can be simulated by forcing the microscopic temperature, energy, or enthalpy to remain fixed.<sup>4</sup>

From the microscopic viewpoint temperature is simply a measure of mean-squared particle velocity. This quantity, when summed over all particles, can be held constant by a frictional damping force  $-\zeta \dot{\mathbf{r}}$ . That additional force, added to the Newtonian Force  $\mathbf{F}$ , can be expressed directly in terms of the interparticle forces and velocities  $\dot{\mathbf{r}}$ :

$$m\ddot{\mathbf{r}} = \mathbf{F} - \zeta \dot{\mathbf{r}} \quad ;$$

$$\zeta \equiv m(\sum \sum \mathbf{F} \cdot \dot{\mathbf{r}}) / (\sum m \dot{\mathbf{r}}^2) \quad ;$$

$$(d/dt)(\sum m \dot{\mathbf{r}}^2) \equiv 0 \quad . \quad (1)$$

The isothermal equations of motion (1) conserve kinetic, rather than total, energy. They can be derived directly from Gauss' "Principle of Least Constraint". This Principle is a generalization of Newtonian mechanics which makes it possible to satisfy constraints (constant temperature, stress, heat flux, ...) typical of nonequilibrium systems. These constrained systems make possible the study of systems with large gradients or flows. For example, under shockwave conditions, "temperature" can be very anisotropic. The temperature parallel to the direction of shockwave propagation can exceed the transverse temperature by a factor of two. Such nonequilibrium temperature distributions can have profound effects on chemical reaction rates. These interesting problems can be treated by a tensor generalization of equation (1), but a thorough discussion would take us too far afield.

With the thermostat provided by equations of motion (1) we can study flow problems involving deformation. The irreversible heat which deformation

provides--viscous heating in fluids, plastic work in solids--can than be absorbed as rapidly as it is produced.

Deformation can be induced through boundary forces or displacements, or by imposing a macroscopic deformation throughout the system. Three types of macroscopic shear deformations are indicated in figure 1:

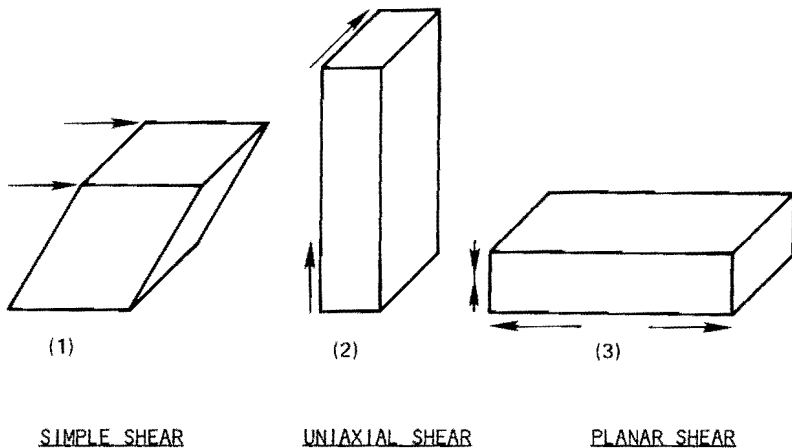


Figure 1. Three Macroscopic Shear Deformations.

In each case the figure shows the effect of deformation on an initial cube. Simple shear (or "plane couette flow") is a rotational flow in which the fluid elements rotate clockwise with an angular velocity equal to half the shear strain rate  $\dot{\epsilon} = du_x/dy$ . Uniaxial shear (with  $\dot{\epsilon}_{xx} = -2\dot{\epsilon}_{yy} = -2\dot{\epsilon}_{zz}$ ) is typical of the shape change undergone during shockwave compression. This flow, as well as the two-dimensional "planar shear" version shown last

(with  $\dot{\epsilon}_{xx} = -\dot{\epsilon}_{yy}; \dot{\epsilon}_{zz} = 0$ ), is irrotational. The first of these flows has been extensively studied, for it can be simulated as a true steady state.

For small strain rates, all three shear flows can be described by the same phenomenological coefficient: shear viscosity in the case of fluids; yield strength in the case of solids. When nonlinear effects must be included, all three flows are fundamentally different. Here we will study in more detail the first flow shown above, simple shear, in the steady state at constant temperature. We will consider a range of strain rates for which nonlinear effects are important.

We begin by distinguishing the systematic macroscopic velocity,  $u = (\dot{\epsilon}y, 0, 0)$ , from the local microscopic velocity  $p/m = (p_x, p_y, p_z)/m$ . We expect that the microscopic velocities  $p/m$  will have nearly an equilibrium (Maxwell-Boltzmann) distribution at small enough rates of strain  $\dot{\epsilon}$ . Because the systematic velocity varies from point to point, there is a Coriolis' acceleration affecting the momenta  $p$ . In the case of simple shear, a free particle moving in the  $y$  direction with  $x$  fixed would undergo an effective acceleration:

$$\ddot{x} = 0 = (p_x/m) + \dot{\epsilon}y \quad \text{-----} \rightarrow \quad \dot{p}_x = -\dot{\epsilon}p_y \quad . \quad (2)$$

Adding this effective acceleration to the Newtonian forces gives the set of equations describing adiabatic simple shear:

$$\begin{aligned} \dot{x} &= (p_x/m) + \dot{\epsilon}y, & \dot{y} &= (p_y/m), & \dot{z} &= (p_z/m), \\ \dot{p}_x &= F_x - \dot{\epsilon}p_y, & \dot{p}_y &= F_y, & \dot{p}_z &= F_z \quad . \end{aligned} \quad (3)$$

Temperature is  $\langle p^2/3mk \rangle$ . By generalizing the friction coefficient  $\zeta$  from (1) to include the Coriolis contribution, we find the equations describing isothermal simple shear:

$$\begin{aligned} \dot{\vec{x}} &= (p_x/m) + \dot{\epsilon}y \quad , \quad \dot{\vec{y}} = (p_y/m) \quad , \quad \dot{\vec{z}} = (p_z/m) \quad , \\ \dot{p}_x &= F_x - \dot{\epsilon}p_y - \zeta p_x \quad , \quad \dot{p}_y = F_y - \zeta p_y \quad , \quad \dot{p}_z = F_z - \zeta p_z \quad . \end{aligned} \quad (4)$$

The boundaries of the system are usually taken to be periodic, as shown<sup>5</sup> in Figure 2, to eliminate the edge effects associated with small systems.

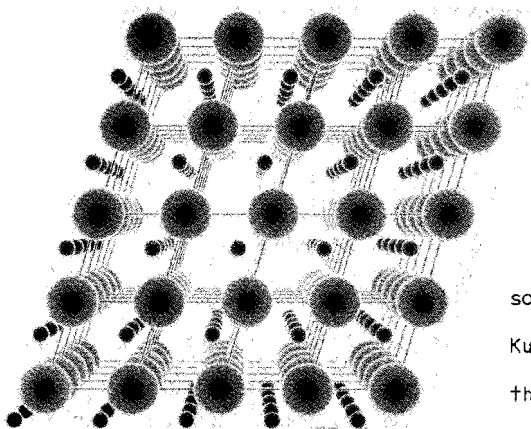


Figure 2. Two-Dimensional Shear Flow.

Shear flow simulations have been carried out for a wide range of thermodynamic states and strain rates, for two- and three-dimensional fluids and solids. In three dimensions there are  $6N$  equations of motion. These can conveniently be solved using the fourth-order Runge-Kutta method. In two dimensions there are  $4N$  equations of motion. The initial velocities are usually chosen from a Maxwell-Boltzmann distribution. The momenta  $\{p\}$  are then scaled to the desired temperature.

That temperature is subsequently maintained by the equations of motion (4). The trajectories which result can then be analyzed for structure.

Thermodynamic functions, such as the pressure tensor, can be obtained by time averaging the corresponding phase functions.

The pressure tensor  $P$  is the same as the momentum flux, a measure of the flow of momentum, per unit area and time. Because the flow direction (normal to the area) and the momentum direction are both vector quantities, pressure is a second-rank (two-index) tensor,  $2 \times 2$  in two dimensions and  $3 \times 3$  in three dimensions. The pressure tensor has two kinds of contributions in a system characterized by pairwise-additive forces. The single-particle convective contributions  $(pp/m)/V$  give the flow of momenta  $p$  across comoving planes oriented normal to the velocities  $p/m$ . In a stationary system with sides  $L_x$ ,  $L_y$ , and  $L_z$ , for instance, the probability that a particle will cross a plane of area  $dA$  perpendicular to the  $x$  axis, during the time interval  $dt$ , is  $(p_x/m)dt dA/V$ . Thus the averaged momentum flow, per unit area and time, is the sum, over all particles, of  $(pp/m)/V$ , with  $V = L_x L_y L_z$ .

There is a second contribution to momentum flux which does not depend upon particle motion, the action-at-a-distance contribution due to inter-particle forces. If particle  $i$ , at  $x_i$ , interacts with particle  $j$ , at  $x_j$ , with the force  $F$ , the probability that a plane normal to the  $x$  axis intersects that interaction is  $\pm(x_i - x_j)dA/V$  and the corresponding flow of momentum per unit time and area is  $\pm F(x_i - x_j)/rdA$ , where  $r$  is the distance separating the two particles. Thus the flow of  $x$  momentum in the  $x$  direction, per unit time and area, has the form  $(x_i - x_j)F(x_i - x_j)/rV$ . The complete pressure tensor  $P$  is the sum of both terms, convective and action-at-a-distance:

$$PV = \sum (pp/m) + \sum \sum rF \quad , \quad (5)$$

where the single sum runs over all particles and the double sum runs over all distinct pairs of particles. If we specify a strain rate  $\dot{\epsilon}$  describing the plane couette flow of Figure 1, the corresponding pressure-tensor element  $P_{xy}$  can then be averaged as a function of time. At sufficiently high rates, in fluids, or even at low rates, in solids,  $P_{xx}$ ,  $P_{yy}$ , and  $P_{zz}$  can also be affected by the shear. These "normal stress effects" are responsible for a host of nonlinear phenomena<sup>6</sup>, two of which are indicated in Figure 3.

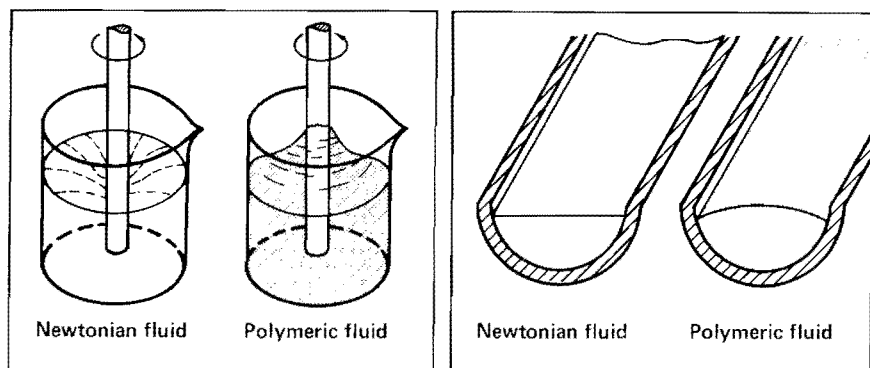


Figure 3. Two Non-Newtonian Flows exhibiting normal-stress effects.

Fluid viscosity is obtained by dividing the shear stress  $-P_{xy}$  by the strain rate  $\dot{\epsilon} = du_x/dy$ . Solid yield strength is simply  $-P_{xy}$ . Both kinds of simulations have been carried out. Some results are described in sections 4 and 6.

#### 4. APPLICATIONS OF NONEQUILIBRIUM MOLECULAR DYNAMICS TO FLUID FLOW

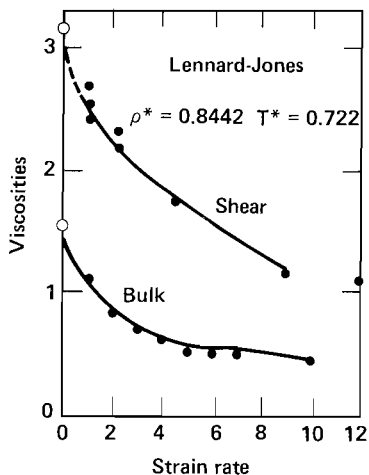


Figure 4. Variation of Viscosities of Liquid Argon with Strain Rate.

and collision diameter are all equal to unity. The extrapolated zero-strain-rate viscosities (open circles) are in good agreement with laboratory measurements.

Laboratory viscosity measurements are relatively straightforward because long-time steady-flow studies can be carried out. Fluid can be forced through a constriction, as in Poiseuille flow, or stirred by a submerged disk. In either case the viscous power loss can be easily measured.

A thorough study of the dependence of shear viscosity on thermodynamic state and strain rate has been carried out, using the Lennard-Jones 6-12 pair potential. Near the freezing line the data depend relatively strongly on strain rate, so that it is necessary to extrapolate from the high rates of the computer simulation to obtain the zero-rate macroscopic value. Typical data<sup>7</sup> are shown in Figure 4. The viscosities and strain rate are given in reduced units: the atomic mass, well depth,

## 5. SHOCKWAVE COMPRESSION

Much larger shear stresses, and higher strain rates, are found in the shockwaves used to compress fluids and solids to high pressures, pressures which can be orders of magnitude higher than the pressure at the center of the earth. The basic shockwave geometry is shown in Figure 5.:



Figure 5. Steady Shockwave Generated by a Piston Compressing a Fluid

In a steady one-dimensional (planar) shockwave cold material is transformed by the shock process into steadily moving hot material with higher pressure, energy, density, and entropy. By measuring the velocities of the moving hot material and the shockwave, it is possible to calculate the final pressure  $P_{xx}$  and energy. For fluids  $P_{xx}$  and the final energy are equilibrium values (because a fluid cannot support shear) and interpretation of the shockwave velocity data is straightforward. For solids  $P_{xx}$  differs from  $P_{yy}$  (the difference is twice the yield strength) and the energy slightly exceeds the value it would have under isotropic conditions. Despite these difficulties, estimates of the solid's shear stress can be made.

## 6. APPLICATIONS OF NONEQUILIBRIUM MOLECULAR DYNAMICS TO PLASTIC FLOW

Shear flow simulations using the equations of motion (4) have also been carried out for solids, both in two and in three dimensions.<sup>8</sup> Although the details of such simulations certainly depend upon the interatomic forces, only one (very simple) force law has been used so far, the piecewise-linear force law shown in Figure 6. This force varies linearly from the force-free separation  $d$  up to a maximum attractive value  $d + w$ . With further stretching the force again decreases linearly to zero at  $r = d + 2w$ .

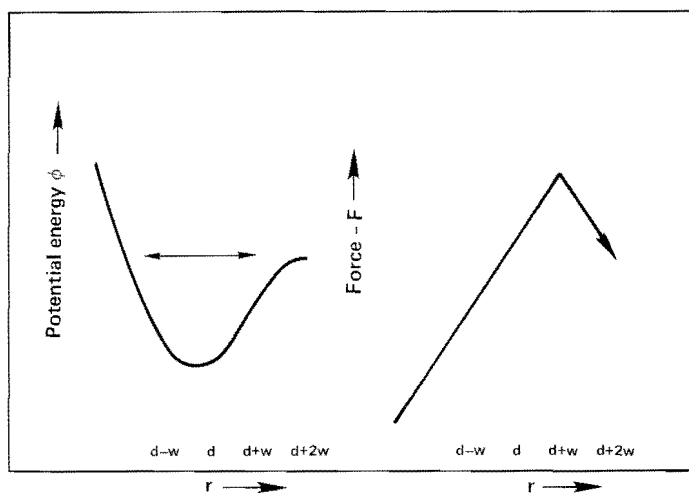


Figure 6. Piecewise-Linear Force Law used in Plasticity Simulations.

In the vicinity of the potential minimum  $d$ , Hooke's Law is obeyed so that crystal properties can be calculated using quasiharmonic lattice dynamics.

That is the main motivation for studying this system. The thermodynamic equation of state, frequency spectrum, and properties of various lattice defects including dislocations, vacancies, and cracks, have all been worked out.

In the case of isothermal steady shear, simulations were carried out for a variety of system sizes, and over about two decades of strain rate, from ten gigahertz to one terahertz. At the low-frequency end of this range, the deforming crystal typically contained only a single pair of dislocations. At the high-frequency end, dislocations were as numerous as particles, so that individual lattice defects could not be identified. The measured dependence of stress (yield strength) on strain rate is summarized in Figure 7.  $G$  is the shear modulus;  $d$  the interparticle spacing; and  $c_T$  is the transverse sound speed.

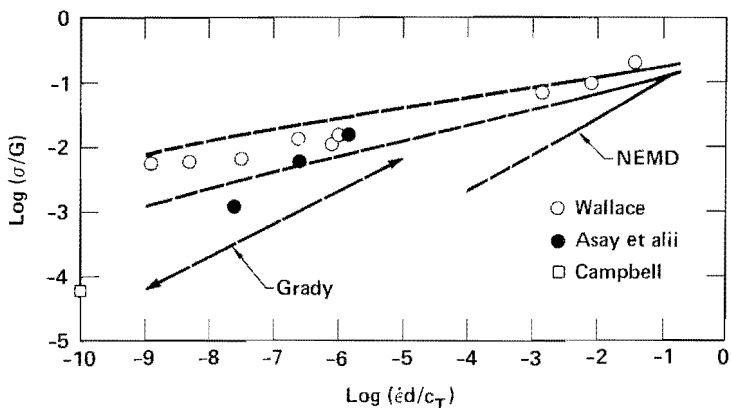


Figure 7. Yield Strength  $\sigma$  (Flow Stress) as a Function of Strain-Rate  $\dot{\epsilon}$ .

The molecular dynamics data lie at the righthand side of the figure. Experimental data, estimates from plastic shockwaves in real metals, appear near the lefthand side of the figure.

The log-log slopes (for three different temperatures) lie between the limits of perfect plasticity (zero slope) and Newtonian Viscosity (unit slope), with the slope increasing linearly with temperature. The correspondence between the computer and laboratory experiments suggests that the same physical mechanism is responsible for both sets of data in the high-strain-rate region.

It seems likely that an understanding of rapid deformation would be useful in interpreting dynamic compaction experiments carried out on powdered amorphous metals. The rapid frictional interactions among the compacting grains certainly lead to terahertz strain rates. The detailed mechanism of the compaction process may thus prove sensitive to rate-dependent plasticity.

## 7. DISLOCATION THEORY OF PLASTIC FLOW

The textbook explanation of plastic flow ascribes that deformation to lattice defects, dislocations, that move through the lattice at speeds somewhat below the transverse sound speed  $c_T$ . Series of simulations of dislocations have been carried out to determine their static and dynamic structure, speed as a function of shear stress, and interaction energy.<sup>3,9</sup> These studies show that the energies of dislocation structures can be adequately described by a pairwise-additive interaction energy of the form predicted by elastic theory. According to the theory, the interaction energy of two dislocations, separated by a distance  $r$  and in the presence of a shear

stress  $\sigma$ , is of the form  $\ln \sigma = -B/\sigma$ , with  $B$  an additive constant. Because the interaction energy has a maximum, Arrhenius kinetics can be used to estimate the rate at which pairs of dislocations are produced, varying as  $\exp(-\Delta E/kT)$ . In the steady state, this rate must equal the annihilation rate, which in turn varies as the square of the strain rate. This equivalence leads to the result that stress must vary as a power of the strain rate:

$$\sigma/\sigma_0 = (\dot{\epsilon}/\dot{\epsilon}_0)^{2kT/Db^2}, \quad (8)$$

where  $D$  is an elastic constant and  $b$  is the interatomic spacing. On the other hand, the molecular dynamics data in figure 7 show conclusively that the 2 in (8) should be replaced by 3, a result impossible to extract from the theory.

#### 8. WHAT REMAINS TO BE DONE?

It is clear that the nonequilibrium simulation methods will prove useful in understanding both experimental data and in advancing the theory of plastic flow in metals. The main difficulties, estimating forces in metals near defects, and understanding the properties of defects when the forces are known (as in computer simulations), still need considerable attention.

## 9. PROBLEM: SAMPLE SIMULATION OF STEADY SHEAR

To illustrate the application of the nonequilibrium equations of motion, we consider an example which is nearly the simplest possible, namely the shear deformation of three particles in two dimensions. Periodic boundaries are used to eliminate edge effects. See Fig. 8.

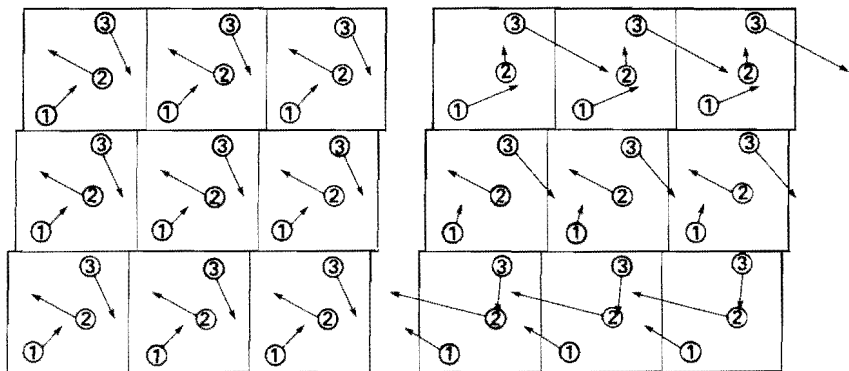


Figure 8. Arrows indicate  $(p/m)$  [left] and  $\dot{r}$  [right].

For convenience we use a truncated Hooke's law force with the force constant, mass, and force-free spring length all set equal to unity. Thus the (purely-repulsive) force has a magnitude  $F = 1 - r$  for  $r < 1$  and  $F = 0$  for  $r > 1$ . Longer-range forces, even forces extending to infinity, can be treated with Ewald's Fourier-transform method, with a moderate increase in computer time. In our sample calculation we choose fixed values of both temperature and strain rate. To start out we specify initial conditions. We choose the time  $t_0 = 0.6$  and the strain rate  $\dot{\epsilon} = 0.1$ , so that the initial shear strain is

0.06, as indicated in Fig. 8. We arbitrarily choose a basic cell of side-length  $L = 2$ . As the calculation proceeds the particle coordinates will eventually leave the central  $2 \times 2$  box. Provided that the accelerations of each particle are based on the nearest images of its two neighbors, as calculated in the three-step process below, it is not necessary to replace the coordinates in the central box. Let us start with the arbitrary set of coordinates  $x, y$  and thermal velocities  $p_x, p_y$  shown in the Table.

Table I. Initial configuration with  $L = 2$  and  $\epsilon = 0.06$  at  $t_0 = 0.6$ .

$i$	1	2	3
$x$	-0.55	+0.21	+0.34
$y$	-0.66	-0.09	+0.75
$p_x$	+0.10	-0.20	+0.10
$p_y$	+0.10	+0.10	-0.20
$F_x$	-0.064	+0.017	+0.047
$F_y$	-0.012	-0.118	+0.130
$i, j$	1,2	2,3	3,1
$y_i - y_j$	-0.57	-0.84	+1.41
$n$	0	0	-1
$y_{ij}$	-0.57	-0.84	-0.59
$x_i - x_j + 2n\epsilon$	-0.76	-0.13	+0.77
$r_{ij}$	0.95	0.85	0.97
$F$	+0.05	+0.15	+0.03

To solve the equations of motion by difference-equation methods we need to calculate the forces on each of the particles. The sheared periodic boundaries must be taken into account in calculating the nearest-image separation of each of the three particle pairs (1,2; 2,3; 3,1). For each (i,j) pair the forces are calculated in three steps:

1. Calculate  $y(i) - y(j)$  and add to it  $nL$ , where  $n$  is the integer chosen to make the final "nearest-image" separation  $y_{ij}$  lie between  $-L/2$  and  $+L/2$ .
2. Calculate  $x(i) - x(j) + nL\dot{\epsilon}t$ , to take into account the offset of periodic images separated by  $nL$  in the  $y$  direction at time  $t$ . Add to this the integer multiple of the box length  $L$  which causes the final nearest-image separation  $x_{ij}$  to lie between  $-L/2$  and  $+L/2$ .
3. Accumulate the  $x$  and  $y$  forces for the nearest-image separation just computed into the forces on  $i$  and the forces on  $j$ . The same numbers are used, with opposite signs.

This force calculation is illustrated in the lower half of the Table. From the forces and thermal velocities the friction coefficient  $\zeta$  can be calculated. For the configuration in the Table, the "friction" coefficient  $\zeta$ , calculated from the forces and momenta according to Gauss' principle:

$$\zeta = m \sum \sum [(F \cdot p/m) - \dot{\epsilon} (p_x p_y/m)] / \sum (p^2/m),$$

is -0.343. In this nonequilibrium problem, where velocities play a direct role in the equations of motion, it is computationally convenient to solve first-order differential equations for particle coordinates and momenta rather than second-order coordinate equations. With the forces and friction coefficient known we have sufficient information to advance the time using a standard first-order differential equation solver. The set of 12 equations corresponding to the homogeneous deformation in Fig. 8 is the following:

$$\begin{aligned} \dot{x}(i) &= [p_x(i)/m] + \dot{\epsilon}y(i) & , & & \dot{y}(i) &= [p_y(i)/m] & , \\ \dot{p}_x(i) &= F_x(i) - \zeta p_x(i) - \dot{\epsilon}p_y(i) & , & & \dot{p}_y(i) &= F_y(i) - \zeta p_y(i) & ; \end{aligned}$$

for  $i = 1, 2,$  and  $3$ . By taking into account the fixed center of mass and fixed kinetic energy these 12 equations could be reduced to seven, but it is simpler to integrate the full set. The inevitable drift in kinetic energy due to finite computational accuracy, can be offset by occasional rescaling of the velocity. Simultaneously, we accumulate the energy and pressure tensor, and the probability distributions in space and velocity. The resulting new configuration, at  $t_0 + dt$ , then replaces the initial condition. We repeat the integration process by returning to step 1 above. Fluctuations in cumulative averages fall off as  $(t - t_0)^{-1/2}$  as the averages stabilize. The shear viscosity is obtained by dividing the long-time steady value of the shear stress  $-P_{xy}$ , by the strain rate  $\dot{\epsilon}$ :  $\eta = -P_{xy}/\dot{\epsilon}$ .

1. W. G. Hoover, Annual Rev. of Phys. Chem. 34, 103 (1983).
2. D. J. Evans, H. J. M. Hanley, and S. Hess, Physics Today 37 (1), 26 (1984).
3. A. J. C. Ladd and W. G. Hoover, Phys. Rev. B 28, 1756 (1983).
4. D. J. Evans, W. G. Hoover, B. H. Failor, B. Moran, and A. J. C. Ladd, Phys. Rev. A 28, 1016 (1983).
5. W. G. Hoover, K. A. Winer, and A. J. C. Ladd, "Irreversibility In the Two-Body Hard-Disk Lorentz Gas", Int. J. of Eng. Sci. (in press).
6. R. B. Bird and C. F. Curtiss, Physics Today 37 (1), 36 (1984).
7. W. G. Hoover, D. J. Evans, R. B. Hickman, A. J. C. Ladd, W. T. Ashurst, and B. Moran, Phys. Rev. A 22, 1690 (1980).
8. W. G. Hoover, A. J. C. Ladd, and B. Moran, Phys. Rev. Letters 48, 1818 (1982).
9. W. G. Hoover, N. E. Hoover, and W. C. Moss, J. Appl. Phys. 50, 829 (1979).